Biointerface Research in Applied Chemistry
Open-Access Journal (ISSN: 2069-5837)

Article,
Volume 13, Issue 2, 2023, 187
https://doi.org/10.33263/BRIAC132.187

Spectroscopic Investigations of Optical Bandgap and Search for Reaction Mechanism Chemistry Due to γ-Rays Irradiated PMMA Polymer

Shiv Govind Prasad [1,2,*], Chhagan Lal [1]

1 Department of Chemistry, School of Basic and Applied Sciences, Harcourt Butler Technical University, Kanpur-208002 UP India; c.lal9940@gmail.com (C.L);
2 Department of Chemistry, Uttar Pradesh Textile Technology Institute, 11/208, Souterganj, Kanpur-208001 UP India; sgp_sinp@yahoo.com (S.G.P.);
* Correspondence sgp_sinp@yahoo.com (S.G.P.);

Scopus Author ID 57202741032
Received: 19.12.2021; Accepted: 16.01.2022; Published: 3.04.2022

Abstract: Radiation damage and the product formation chemistry in Polymethyl methacrylate (PMMA) due to γ-irradiation have been studied by SEM, XRD, FTIR, and UV-Vis spectroscopy. Co-60 gamma source with a dose rate of 1.707 kGy/hr has been used for irradiation to a total 570 kGy dose. No significant changes in morphology upon such irradiation. Crystallinity decreases at a lower dose and then increases for a higher dose. Crosslinking dominates at lower doses, and chain scission overwhelms at higher doses in the irradiated polymer. Two isosbestic points are formed, and the absorption maxima shift towards a higher wavelength. The optical bandgap energy decreases with the addition of radiation dose. A new FTIR peak at 1638 cm-1 appeared, suggesting the formation of an unsaturation center in the irradiated polymer. Up to a dose of 409 kGy, FTIR absorption peak intensity increases and decreases with further irradiation.

Keywords: FTIR; UV-Vis spectroscopy; PMMA; SEM; XRD; polymer; isosbestic point; gamma radiation; reaction mechanism.

© 2022 by the authors. This article is an open-access article distributed under the terms and conditions of the Creative Commons Attribution (CC BY) license (https://creativecommons.org/licenses/by/4.0/).

1. Introduction

Polymethyl methacrylate (PMMA) is an amorphous, transparent, and colorless thermoplastic material having good abrasion, UV resistance, and solvent resistance properties. It is also known as Diakon, Lucite, Oroglas, Perspex, Plexiglas. PMMA in science and technology, particularly in optics, electronics, biotechnology, photonics, space research, and radiation shielding, in pure and composite forms, is well documented [1-18]. Polymer properties can be modified by irradiation with ionizing radiations: x-ray, gamma radiation, and electron & ion beams [19-28]. High energy ionizing radiation loses energy by inelastic interaction with a polymeric material [29]. The changes in polymer properties generally depend on radiation dose, internal polymer structure, length of chain, and the functional groups present in the polymer [30-33]. The properties of the polymeric materials mainly depend upon the formation of the crosslinking and chain scission. There is a competition between chain scission and crosslinking during irradiation, controlled by the structural properties of the polymer [34]. It is a well-established fact that various types of chemical changes take place in the polymers

during irradiation, such as elimination of low molecular weight products (H_2, CO, CO_2), [35-37] formation of vacancy clusters, generation of color centers, main chain scission in the polymer molecules leads to decrease of its molecular weight, creation of new unsaturated bonds and radical-radical combination (crosslinking with an increase in molecular weight) [38-41].

The effects of radiation on PMMA polymer have been studied by a number of researchers, including the solid polymer of gamma-irradiated PMMA contains long-lived free radicals, as described by [42-43], depolymerization [44] is the preeminence reaction in the thermal degradation of PMMA polymers, with volatile product formation [35,36] is observed in irradiated PMMA. The absorption of moisture and dimerization of the carbonyl group in gamma-irradiated PMMA film is reported [2]. Positron annihilation lifetime spectroscopy (PAL) [19] showed that the size and amount of free volume decrease with increasing radiation dose due to irradiation-enhanced crosslinking in a polymer. The gamma-irradiated PMMA-Reduced Graphene Oxide composite films can be an excellent candidate for biosensing and biomedical applications [45-47]. PMMA film rupture [48] caused by irradiation occurred before the start of the carbonization of the irradiated area. The gamma radiation modifies the polymeric material's surface morphology and optical property [49].

The radiation chemistry of PMMA, after gamma irradiation, is of great technological importance to find out mechanisms of chain scission and to crosslink in an irradiated polymer. Although various published papers on gamma radiation damage in PMMA polymer are reported [2,7,8,10,17,19,28,33,37,49], the damage mechanism is still not well understood. The damages have been estimated using a scanning electron microscope (SEM), ultraviolet-visible spectrophotometer, Fourier Transform Infrared (FTIR) Spectrometer, and X-rays diffractometer. The bandgap energy (E_g) has been derived from optical absorption spectra. The present work discusses schematic reaction mechanisms of product formation chemistry. Empirical, experimental data on the behavior of gamma-irradiated PMMA have been interpreted in terms of absorbed dose.

2. Materials and Methods

2.1. Materials and irradiation.

PMMA is an amorphous and transparent thermoplastic polymer. PMMA sheets of 0.38 mm thickness, procured from Good fellow Cambridge Limited, England, have been used without further treatment. Samples of size 2×3 cm^2 have been cut manually from the PMMA sheet. Radiation damage in the polymer is greatly affected by the extent of the dose rate. Irradiation is carried out with a dose rate of 1.707 kGy/hr using a ^{60}Co-gamma source at UGC-DAE CSR, Kolkata, W.B. India, with doses up to the maximum dose of 570 kGy. The general chemical structure of PMMA is shown in Figure 1, and the camera view of pristine and irradiated polymer is shown in Figure 2, respectively.

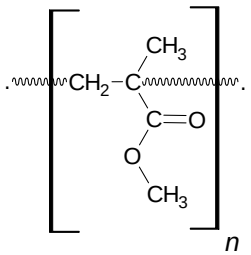

Figure 1. Chemical structure of PMMA polymer.

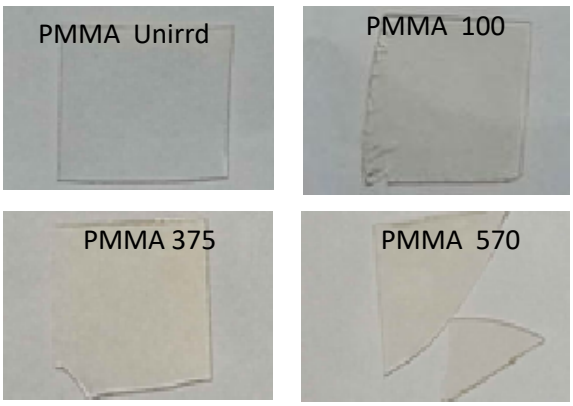

Figure 2. Camera view of unirradiated and 100kGy, 375kGy, and 570 kGy irradiated PMMA polymer.

2.2. Characterization.

2.2.1. X-ray diffraction.

The XRD measurement has been done with PROTO, AXRD Benchtop Powder Diffraction system using monochromatic CuKα (λ=1.541Å) line over 2θ set from 10º to 70º. The operating conditions were voltage 27 kV and current 12mA. For XRD, each sample has been mounted on the spinning sample-holder, using clay to maintain the height of the polymer sheet. The XRD patterns of pristine or unirradiated and different irradiated PMMA polymers are shown in Figure 3.

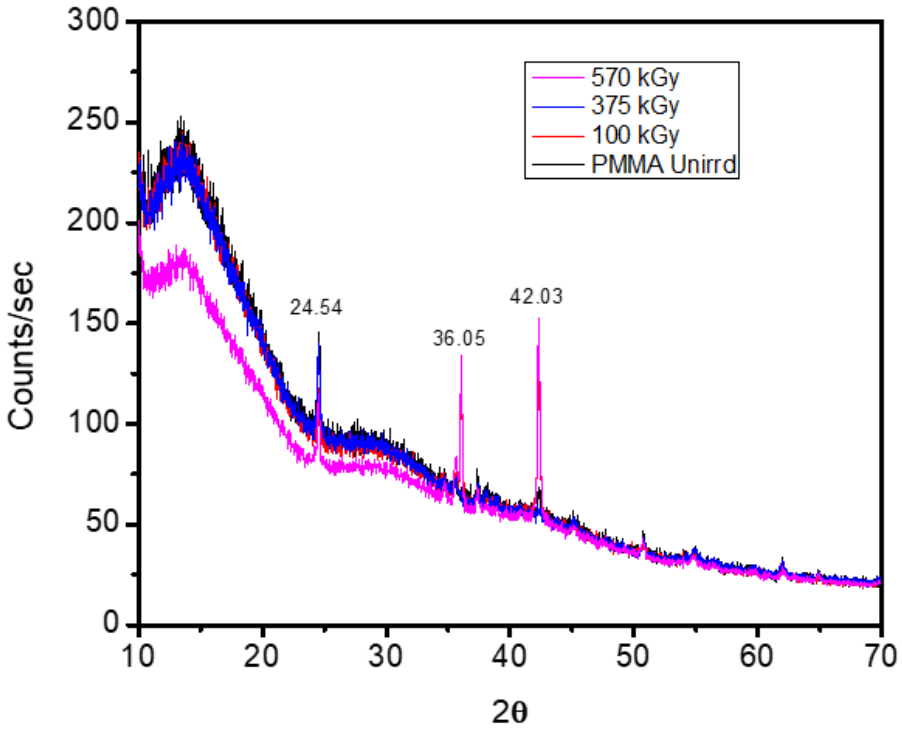

Figure 3. XRD patterns of unirradiated and gamma-irradiated PMMA polymer.

2.2.2. Scanning Electron Microscopy (SEM).

The surface morphology of gamma-irradiated and pristine or unirradiated PMMA samples were also examined using a scanning electron microscope (JEOL: JCM- 7000 Benchtop SEM). The SEM images were used to study the morphological characteristics of PMMA films before and after irradiation with the various gamma doses are shown in Figure 4.

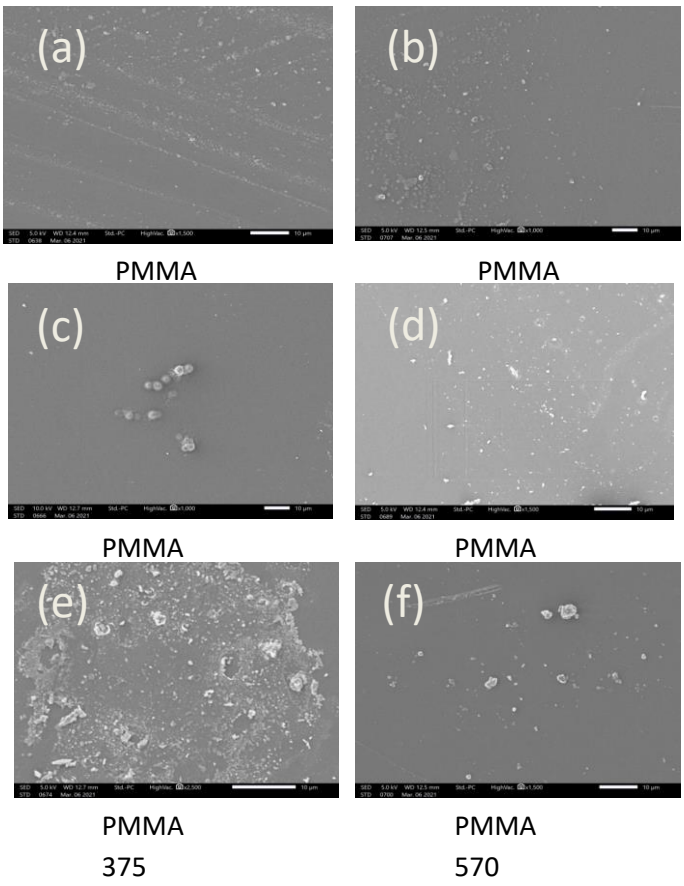

Figure 4. SEM image of PMMA (**a**) pristine; (**b**) 48 kGy; (**c**) 160 kGy; (**d**) 280 kGy; (**e**) 375 kGy; (**f**) 570 kGy.

2.2.3. UV-Visible spectrometry.

Optical absorption spectra of pristine and irradiated samples were measured in the wavelength range 200-1100 nm, in absorption mode, using a step size of 0.5 nm, in UV-Vis spectrophotometer (Lambda 360, India). The UV-Visible absorption spectra of pristine and various gamma dose irradiated samples have been shown in Figure 5, in the 200 -600 nm wavelength range.

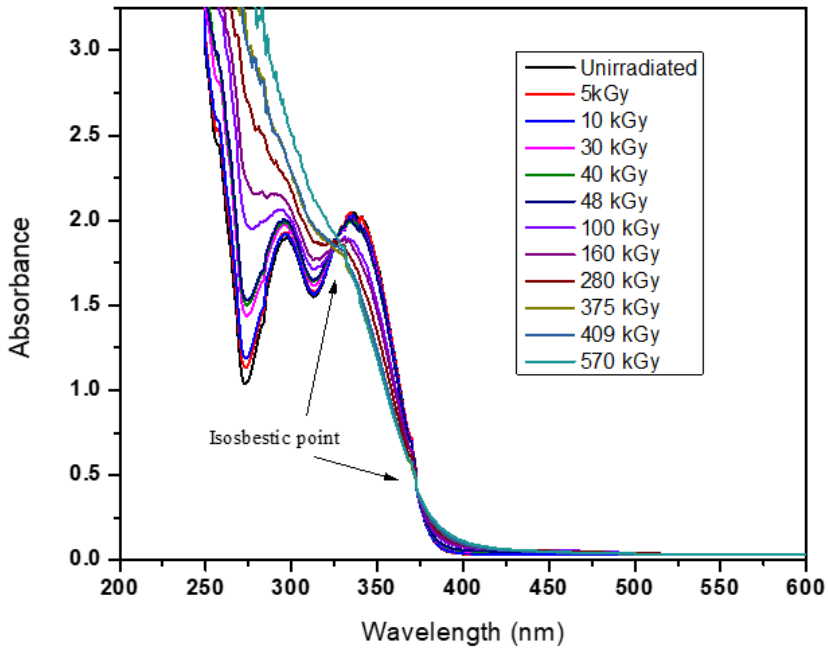

Figure 5. UV-Visible absorption spectra of pristine and gamma-irradiated PMMA polymer.

2.2.4. FTIR Spectrometry.

FTIR spectra of virgin and each irradiated sample were recorded in the wavenumber range 600 to 4000 cm^{-1} in transmission mode using attenuated total reflection (ATR) facility in Alpha-model FTIR spectrometer of Bruker, Germany. FTIR spectra of pristine and gamma-irradiated PMMA polymer are shown in Figure 6.

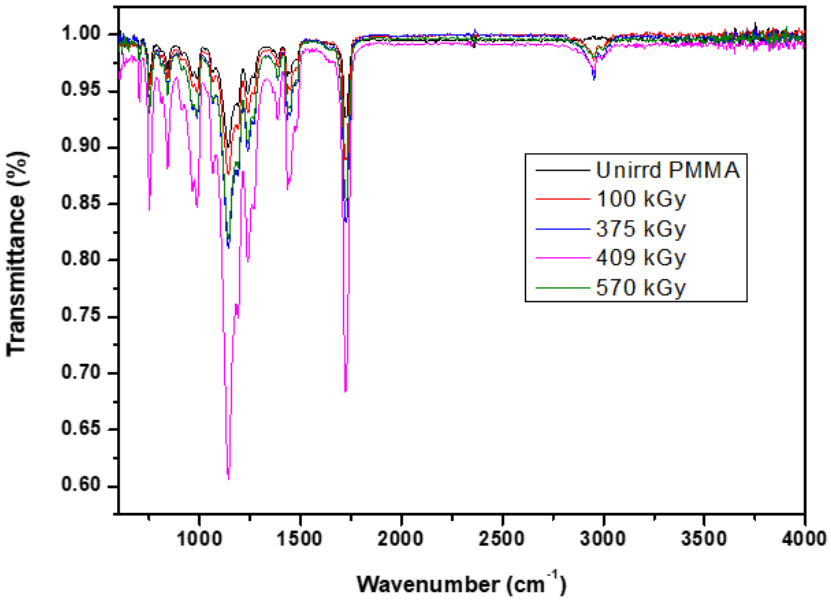

Figure 6. FTIR spectrum of pristine and different gamma dose irradiated PMMA polymer.

3. Results and Discussion

3.1. XRD.

The calculated distance between lattice planes (d-spacing) values, crystallite size, and crystallinity percentage have been shown in Table 1 from the X-Ray diffraction (XRD) pattern using Bragg's equation: $d= \lambda/2\sin\theta$, where λ is the wavelength of X-ray used, and 2θ is the diffraction angle. The full width at half maximum (FWHM) of the diffraction peak was calculated by fitting the XRD data, and the crystallite size (L) was estimated by using the Scherrer equation: $L= K\lambda /\beta \cos\theta$, where K is Scherrer constant, which depends upon lattice direction and crystallite morphology, and β is the FWHM.

Table 1. Calculated lattice planes (d-spacing) values, crystallite size, and crystallinity percentage for pristine and gamma-irradiated PMMA polymer samples.

PMMA sample	2θ	β = FWHM	Crystallite size (*L*) nm	d (nm)	Crystallinity (%)	Amorphous (%)
Unirrad	24.56	0.21624	371.90	36.2266	56.60	43.40
100 kGy	24.50	0.19260	417.50	36.3139	54.08	45.92
375 kGy	24.54	0.24031	334.62	36.2847	54.38	45.62
570 kGy	24.54	0.23107	348.01	36.2847	57.02	42.98

From Table 1, it has been observed that there is no significant effect of radiation on the distance between the lattice planes for the total dose of 570 kGy. The crystallite size initially increases for 100 kGy doses and decreases with an increase in radiation dose. This seems to be that radiation induces both chain scission and crosslinking phenomena in in the irradiated polymer. At a lower dose, it was crosslinking dominates over chain scission behavior. However, with an increase in radiation dose, chain scission predominates over crosslinking in

irradiated PMMA polymer. The crystallinity initially decreases, which moderately increases on a further dose increase. This is because the generation of free radicals and the formation of crosslinking restrict the motion of the polymer chain, and hence the building of disorder (amorphous regions) takes place. At the higher dose of 570 kGy, chain scission predominates over crosslinking in irradiated PMMA polymer. This is because chain scission provides extra mobility to the polymer chains to crystallize, increasing the crystallinity.

3.2. SEM.

From the SEM image of the PMMA films before irradiation, as shown in Figure 4, one can note that irradiation revealed that no noticeable changes were observed in the morphology after irradiation. At 160 kGy gamma-irradiated images (Figure 4c) show the diffusion of gas bubbles coming out from the surface. Irradiation up to 570 kGy does not offer any remarkable effect on the morphological characteristics of the PMMA sheet. There is a report reveals that a lower dose of irradiation did not influence the morphological characteristics of polymeric materials [50].

3.3. UV visible spectroscopy.

As shown in Figure 5 of pristine and the irradiated PMMA polymer, the UV-visible absorption spectrum is recorded in the wavelength range of 200-1100 nm at room temperature and is more sensitive in the 250-550 nm wavelength regions. Details of the spectra are given in the proceeding text.

3.3.1. Region between 250-325 nm.

The absorption value in the range of 250-325 nm is due to the $\pi \rightarrow \pi^*$ transition. It has been noticed that the absorbance value increases with the increase in gamma irradiation dose. On irradiation, the nature of spectra is modified, and optical density (absorption value) increases. This is due to the detachment of more methyl carboxylate radicals (CH_3OCO) [51] and the change in the chemical structure of the irradiated polymer on increasing the radiation dose. This increase in absorption value infers an increase in density of the chromophores within the polymer sample that allow $\pi \rightarrow \pi^*$ transitions due to the formation of sequential (–C=C–) unsaturated centers in the main polymer chain.

3.3.2. Region between 325-375 nm.

The absorption value in the range of 325-375 nm is decreased with an increase in the irradiation dose. This suggests that the chemical structure in the >C=O system is changed after irradiation. It is due to the decomposition of unimolecular methyl carboxylate radicals (CH_3OCO) formed from the detachment of PMMA polymer. These methyl carboxylate radicals break into small molecular weight products of carbon dioxide [51-52]; as a result, absorbance decreases.

3.3.3. Region between 375-540 nm.

The absorption value in the range of 375-540 nm is due to the $n \rightarrow \pi^*$ transition in the carbonyl (>C=O) system. It has been seen that the absorbance value increases with the increase in gamma irradiation dose. It is attributed to the irradiation-inducing unsaturated center in the

form of conjugated dienes $(-C=C-)_n$ group in the irradiated PMMA polymer chain [2,28,30,34,53]. An increase in the density of the unsaturated dienes group in the irradiated polymer can increase the absorption over the broad spectral range from 250-375 nm.

It has been submitted that the formation of a new band from 375 to 540 nm is due to the presence of color centers in the polymer sample. This is due to the generation of radicals and the development of vacancies inside the tracks of the polymer. Therefore, the trapping of electrons and holes under irradiation occurs. Furthermore, the absorbance value of the color center band increases on irradiation. This seems to be due to the generation of radicals resulting from chain scission in the polymer. The chain scission improves the mobility of the polymer chains and reduces crosslinking.

3.3.4. Isosbestic points.

We have found that in the absorption spectra (Figure 5), two isosbestic points (at wavelength 325 nm & 373 nm) are developed, at which these absorption spectra cross each other. Isosbestic point is a specific wavelength or frequency at which the absorbance of a material does not change during a physical change or a chemical reaction in the sample. The transparency of a material is directly related to the amorphous portion of polymer material. Absorbance is wavelength-dependent material properties [54] and depends solely on the absorption and transmission coefficient ratio. The two isosbestic points are developed because at wavelength 325 nm and 373 nm, the absorption and transmission coefficient is counterbalancing to each other so that the absorbance value remains unchanged.

3.3.5. Optical bandgap.

According to Tauc and Davis–Mott model [55], the shift in absorption edge from ultraviolet towards visible region under irradiation was correlated with E_g (the bandgap energy) as follows: $\alpha h\nu = B^2(h\nu - E_g)^m$, where $\alpha = 2.303A/d$, with A = absorbance and d = thickness of the sample.

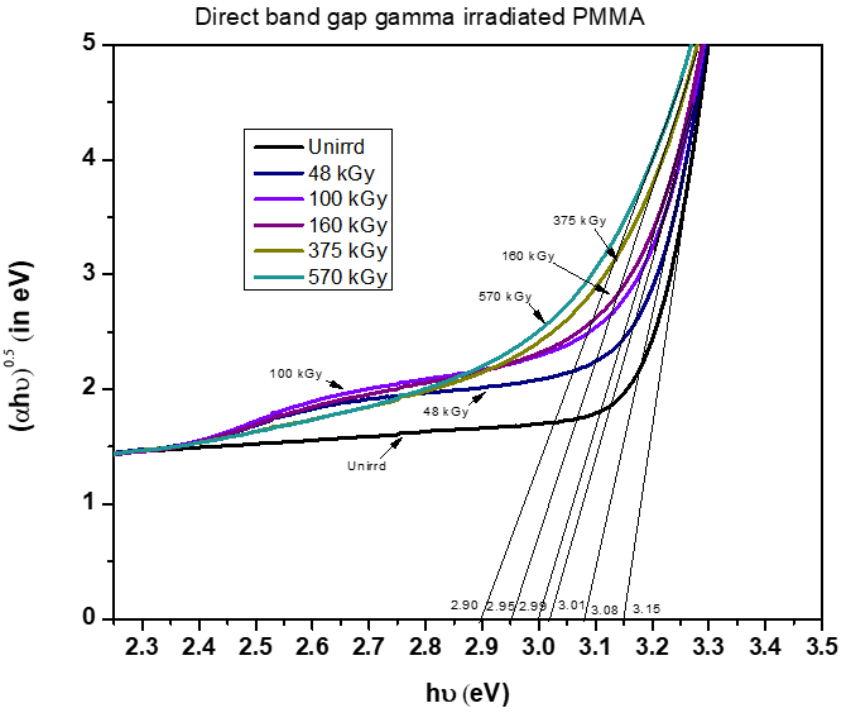

Figure 7. Bandgap energy evaluation of pristine and gamma-irradiated PMMA polymer.

Also, α is the optical absorption coefficient, and ν = c/λ is the frequency of incident photon (with λ=wavelength & c= velocity of light in vacuum), h = Plank constant, B = band tailing parameter. B (depending on transition probability) has been assumed to be constant in the optical frequency range. Here, m is the transition index parameter. It may have values (2, 3, 1/2, and 1/3), implying indirect allowed, indirect forbidden, direct allowed, and directly forbidden transitions, respectively [56, 57]. We have estimated the bandgap (E_g) as shown in Figure 7 and Table 2, using equation $\alpha h\nu = B^2(h\nu - E_g)^m$.

Table 2. Compilation of Tauc and Davis–Mott model [$\alpha h\nu = B^2(h\nu - E_g)^m$] fit parameters for bandgap energy (E_g) and absorption edge (λ_g) parameter (here, m = ½ for directly allowed band gap) for the PMMA samples irradiated with different gamma doses.

Gamma Irradiation dose in (kGy)	Unirrd.	48	100	160	375	570
Bandgap energy (E_g) in (eV)	3.15	3.08	3.01	2.99	2.95	2.90
Absorption edge (λ_g) in (nm)	394	403	412	415	420	428

In general, ionizing radiations create defects and/or enriched carbon clusters, removing low molecular weight volatile products in the polymer due to this material's bandgap modifies. [21, 29, 34-36, 38, 58-61]. From Table 2, it is noticed that the bandgap energy of PMMA polymer decreases with an increase in gamma dose. This decrease in the bandgap energy is due to the generation of defects in the irradiated PMMA. Consequently, this bond-breaking might lead to a lower energy state in the irradiated polymer. It is reported that change in bandgap seems to be due to the phenomenon of chain scission and crosslinking [2]. On increasing radiation from a lower dose (100 kGy) to a higher one, chain scission dominates over crosslinking. This induces an increase in the polymer chain flexibility, and a decrease in the bandgap is observed.

The formation of isosbestic points suggests the rearrangement of polymer chains occurs in the impact of the energy transfer. This transfer of energy alters the irradiated polymer so that at wavelengths 325 nm and 373 nm, the absorbance of light is negligible. There are reports [2,58] that suggest that the magnitude of crosslinking and chain scission mainly depends on the structure of the polymer [62].

Here, the availability of many PMMA molecules for the chain scission and the radicals for the crosslinking increases the absorption amplitude.

3.4. FTIR spectroscopy.

FTIR analysis was used to investigate the nature of the chemical modifications caused by gamma irradiation in PMMA. The spectra of the gamma-irradiated PMMA polymer (refer to Figure 6) are nearly similar to that of the pristine PMMA except for changes in the amplitude and the locations of absorption peaks. The position of characteristics absorptions observed in FTIR spectra is presented in Table 3. It has been observed that the absorption intensity of most of the peaks in FTIR spectra increases after gamma irradiation up to 409 kGy, followed by decreases up to dose 570 kGy.

The FTIR spectra peaks at 2950 and 2996 cm^{-1} show an intense C-H symmetric and asymmetric stretching. Attributed to the C-H stretching vibrations in carbonyl OCH_3, pendent CH_3, and primary chain $–CH_2–$ group [2,34,63]. The broad peak of the C-H vibration mode is due to pendant methyl groups influenced by neighboring chains' methyl groups [61]. The peak at 1726 cm^{-1} is attributed to the ester carbonyl group (>C=O) stretching vibrations, which is found in agreement with the earlier reported results [2,30,34, 51,52, 63-64]. Band peak below

1500 cm^{-1} shows many peaks is due to the C-H deformation mode of methyl subunit between 1500 cm^{-1} and 1385 cm^{-1}. The peak between 1237 and 1268 cm^{-1} is attributed to C-C-O stretching vibrations of the methyl carbonyl group. Moreover, the peak between 1190 and 1141 cm^{-1} is due to C-O-C vibrations. The peaks 911, 964, and 985 cm^{-1} have been assigned for C-H rocking modes, and 751cm^{-1} assigned for C-C skeletal mode [2,51].

Table 3. FTIR peaks (peak in cm^{-1}) assignment for pristine and gamma-irradiated PMMA polymer.

Pristine	100 kGy	375 kGy	409 kGy	570 kGy	Wave number & Reference
751	751	751	751	751	751, C-C stretch, C-C skeletal mode [2,51,52, 63,64]
839	841	841	841	841	839, CH_2 rocking, [2,51,52, 63,64]
911	909	915	913	915	911, O-CH_3 rock[2,51,52, 63,64]
964	966	966	964	968	964, O-CH_3 rock [2,51,52, 63,64]
985	985	985	985	985	985, O-CH_3 rock [2,51,52, 63,64]
1065	1063	1063	1065	1063	1065,C-O-C Asymmetric stretching, [2,51,52, 63,64]
1141	1141	1141	1141	1141	1141, C-O-C Asymmetric stretching, [2,51,52, 63,64]
1190	1190	1190	1190	1190	1190, C-O-C Asymmetric stretching, [2,51,52, 63,64]
1237	1239	1239	1237	1237	1237, C-C-O Symmetric stretching, [2,51,52, 63,64]
1268	1268	1268	1268	1268	1268, C-C-O Symmetric stretching, [2,51,52, 63,64]
1385	1385	1385	1385	1385	1385, C-H deformation, (C-H bending), [2,51,52, 63,64]
1434	1434	1434	1434	1434	1434, C-H deformation, (C-CH_3 bending, C-CH_2-bending), [2,51,52, 63,64]
-	1640	1640	1638	1640	1635, (broad), C=CH_2 stretching (in α,β unsaturated carbonyl compound), [2,51,52, 63,64]
1726	1724	1724	1720	1726	1726, C=O stretching[2,30,34, 51,52, 63,64]
2358	2362	2358	2344	2364	2358 (free CO_2) [63-64]
-	2951	2951	2951	2949	2950, C-H Symmetric stretching in –CH_2–, –CH_3 and –CH_2– [2, 27-30,34,51,52, 63,64]
-	2998	2992	2996	2996	2996, C-H Asymmetric stretching in (–CH_2–, –CH_3 and –CH_2– [2, 27-30,34, 51,52, 63,64]
-	-	-	3651	3649	3651, O-H stretching [2,51,52, 63,64]

Gamma radiation up to 409 kGy enhances the absorption intensity of most of the peaks in the spectra, followed by a decrease in its intensity at higher doses of 570 kGy. The carbonyl group peak shifted from 1726 cm^{-1} to a new position at 1722 cm^{-1} and changed its amplitude. The peak intensity below 1300 cm^{-1} increases up to 409 kGy irradiation. Significant broadband between 3300 and 3750 cm^{-1} is observed due to the formation of the hydroxyl group. In ion irradiation, hydroxyl group formation was reported by many researchers [51,52,63,64]. The development of hydroxyl group formation is explained in (eq. no 15) schematic presentation of the reaction mechanism.

The new peak at 1640 cm^{-1} was observed and attributed to an unsaturated (C=C) stretching vibration. Its intensity increased, and the peak shifted to 1638cm^{-1} for up to dose 409 kGy. At a higher radiation dose of 570 kGy, peak intensity decreased and moved to 1640 cm^{-1}. In pristine PMMA polymer absence of a 1640 cm^{-1} is peak suggests no formation of the unsaturated group (-C=C-) in the polymer. The increase in peak intensity indicates that more unsaturated groups are created, and the shifting of the peak in a lower position from 1640 to 1638 cm^{-1} suggests conjugation formation [2,51,52, 63,64]. Broadening of peak around 1640 cm^{-1} means a different type of environment for (C=C) group. Formation of unsaturation is explained in schematic reactions (5,6,9) presentation of the reaction mechanism.

The absorption peak corresponding to carbonyl group (>C=O) vibration occurs in pristine PMMA sample at 1726 cm^{-1}, whereas in 409 kGy gamma-irradiated samples, it appears at 1720 cm^{-1} with the increase in intensity. This suggests that the carbonyl group environment

being changed and peak shift to the lower value is due to the carbonyl group existing in the conjugated environment. The formation of the carbonyl group (>C=O) is explained in the schematic reactions (9,11,14) presentation of the reaction mechanism.

It has been noticed that the maximum increase in the absorption for 1638 and 1726 cm^{-1} peaks after 409 kGy irradiation, followed by a decrease in intensity for higher doses. This is probably due to the generation of more methyl carboxylate radicals (CH_3OCO) [51] and the formation of an unsaturation center (defects). On further irradiation (up to 570 kGy), a decrease in absorbance value suggests a more radical combination involved. As a consequence decrease in absorption is observed. The long polymer molecular chain breaks and links among the leading chains through radical coupling (crosslinking) that occurs in the irradiated polymer. Breaking the molecular chain is more than crosslinking in case of a higher dose. The absorption becomes lower at a higher dose is due to the fragmentation of the subunit methyl carboxylate radicals into low molecular weight CO and CO_2 volatile products. This suppresses the intensity of the carbonyl group. The decrease in intensity with an increase of radiation dose from 409 to 570 kGy as observed in peaks at 751, 1141, 1239, and 1726 cm^{-1} to a negative direction indicates the breaking of C-C, C-O-C, and C-C-O bonds [2].

It assumed the band at 1638 cm^{-1} occurs due to the generation of unsaturation as a result of the recombination of the radicals. Negligible change in the intensity of the peak at ~2358 cm^{-1} (attributed to free CO_2) indicates the insignificant amount of CO_2 gas evolved in the present case. However, SEM images (Figure 4 c) support the evolution of gas formation. The formation of a small molecule CO and CO_2 is explained in the scheme of reaction (2) presentation of the reaction mechanism. Small-molecule CO, CO_2 is formed due to chain scission dominance over crosslinking at a higher dose.

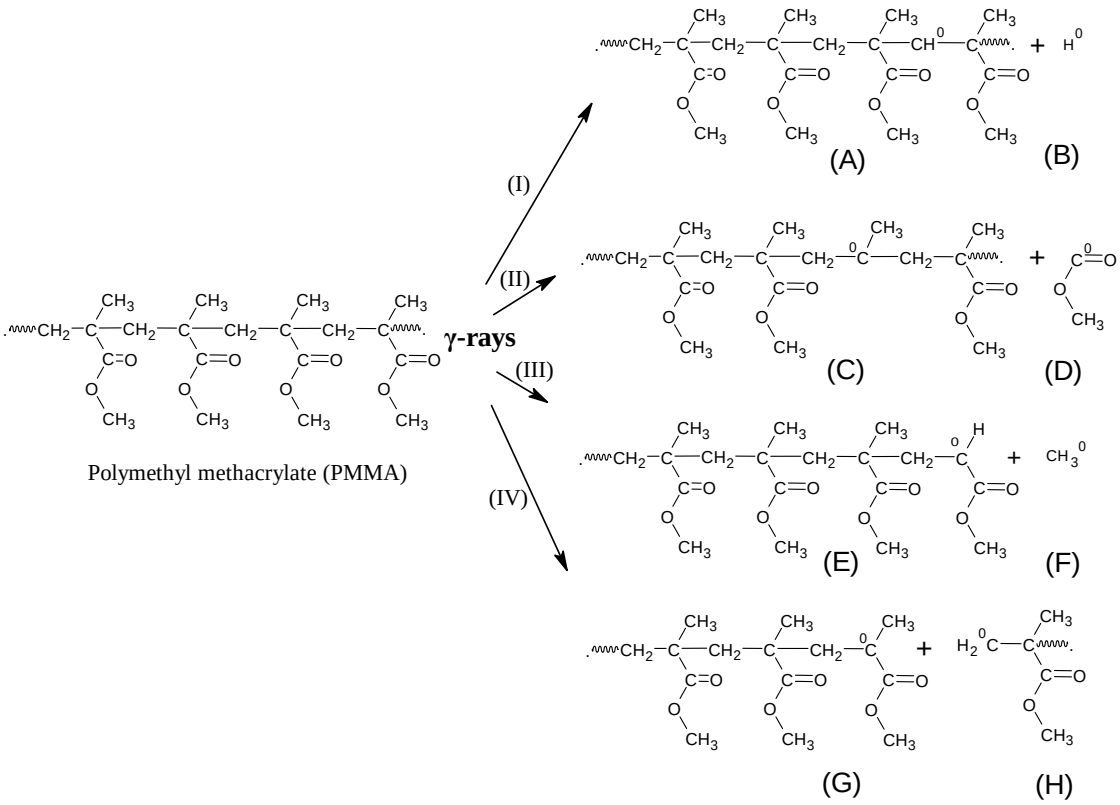

Polymethyl methacrylate (PMMA)

Generation of free radicals A, B, C, D, E, F, G & H in irradiated PMMA -- (1)

3.5. Schematic reaction mechanism of product formation.

The ionization and excitation phenomena occur within the polymer when electromagnetic radiation (ionizing radiation) interacts. This is due to the transfer of energy to the polymer molecules of the medium. Due to this, polymers endure bond cleavages after absorbing energy, resulting in the formation of non-saturated fragments called free radicals [58]. These free radicals are responsible for most chemical transformations reaction (I, II, III & IV), as shown in the following reaction scheme (1).

3.5.1. Generation of free radical, liberation of low molecular weight species.

The low molecular weight free radicals (B, D, F) formed in the scheme of reaction (1) go into the radical-radical coupling and produce a low molecular weight stable volatile product, as shown in the following scheme of reaction (2).

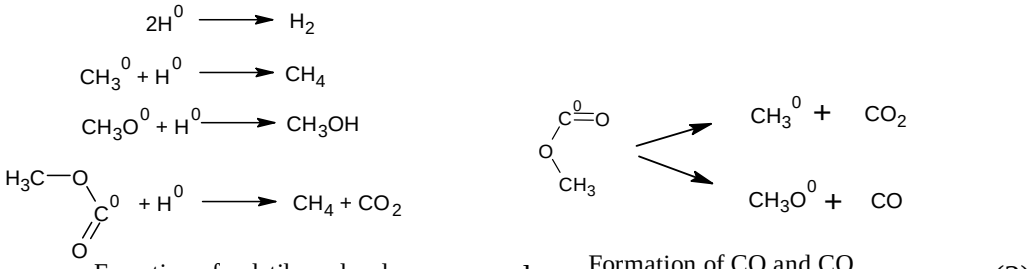

-- (2)

3.5.2. Dimerization (radical coupling).

The bond dissociation energy for the tertiary C-H bond is much less than that of the secondary and primary C-H bonds.

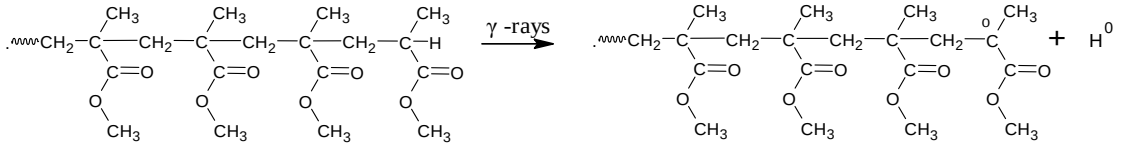

-- (3)

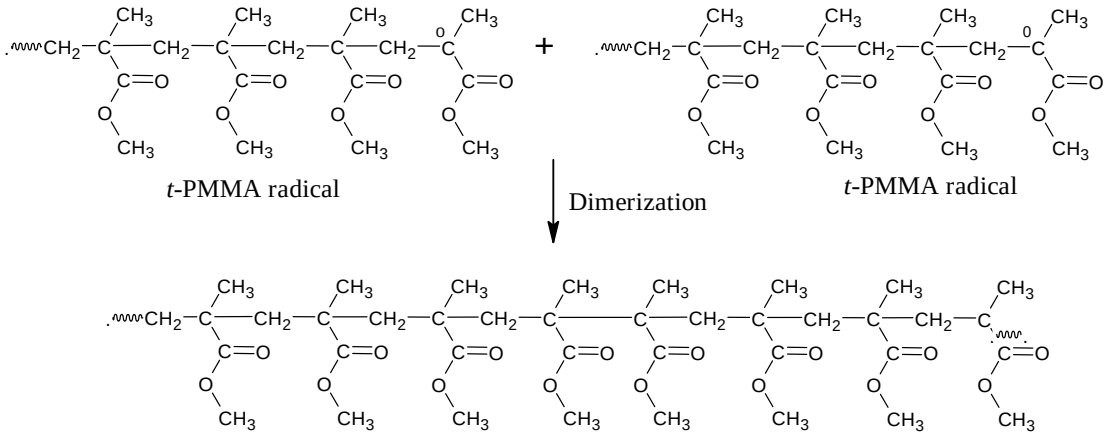

-- (4)

The weak C-H bond in the tertiary compound is the most preferred dissociation of PMMA polymer that generates the highly unstable PMMA radical. This unstable radical is

dimerized into a PMMA-PMMA type dimer compound, as shown in the scheme of reactions (3) & (4). This agrees with the report of dimer formation in PMMA [65].

3.5.3. Formation of unsaturation and color center.

Irradiation at first cleaves the C-H bond and occurs in the scheme of reaction (I), leading to unstable hydrogen free radicals. Consequently, the unstable C-C bond undergoes pendent group cleavage ($OCOCH_3$ and CH_3), as shown in the scheme of reactions (5) & (6), resulting in the formation of molecular fragments with one of the fragments containing C=C at the side chain. The formation of these extended conjugation double bonds in the scheme of reaction (5) within the irradiated sample is one of the reasons for the change in color of the film from white to pale yellow (Figure 2).

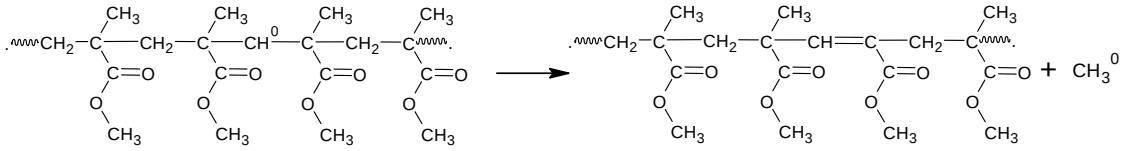

PMMA in radical form — Formation of conjugated unsaturation (color) -- (5)

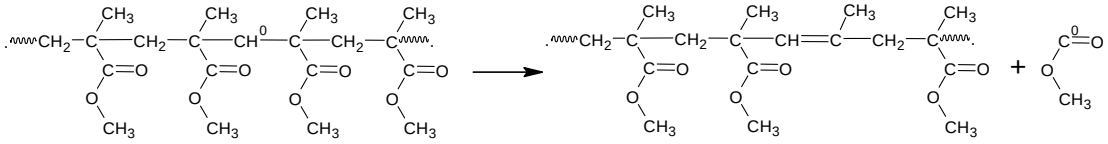

PMMA in radical form — Non conjugated unsaturation formation -- (6)

3.5.4. Formation crosslinking.

Irradiation at first cleaves the C-H bond occurs in the scheme of reaction (I), leading to unstable two or more hydrogen free radicals, undergoes crosslinking as shown in the scheme of reactions (7) and (8).

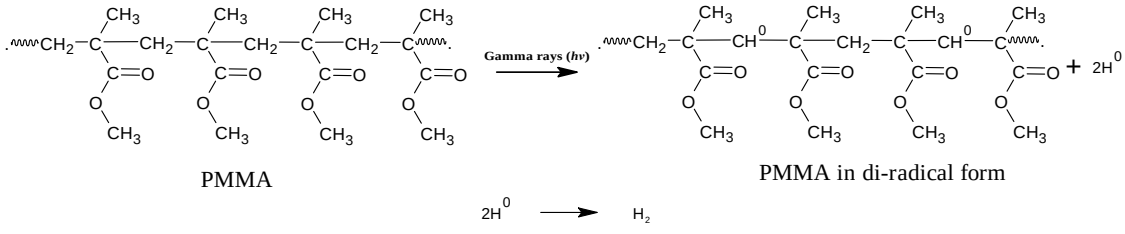

PMMA — PMMA in di-radical form

$2H^0 \longrightarrow H_2$ -- (7)

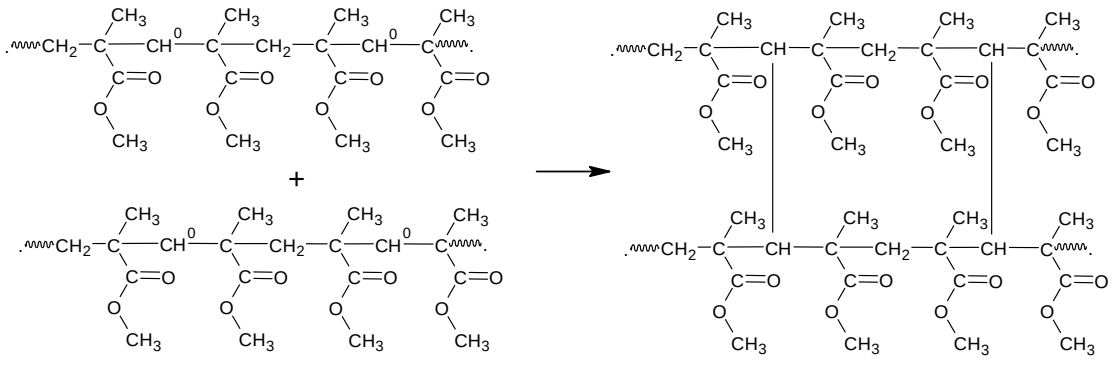

PMMA in di-radical form — Cross-linking formation -- (8)

3.5.5. Formation of chain scission, depolymerization.

The radical formed in the scheme of reaction (I), leading to the C-C bond cleavage, undergoes main chain scission as shown in the scheme of reactions (9), (10), and (11)—resulting in the formation of molecular fragments with one of the fragments containing C=C at the side chain. The depolymerization of PMMA polymer into monomer is explained in the scheme of reactions (10) and (11). This agrees with the result reported by [44].

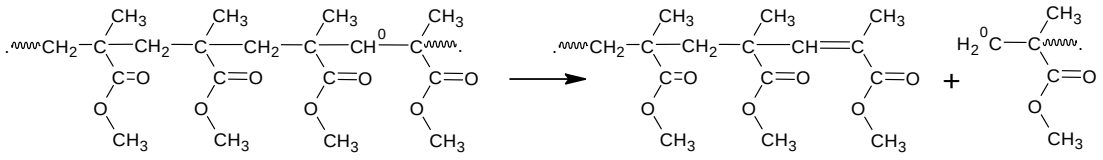

PMMA in radical form — Formation of unsaturation — Chain scission -- (9)

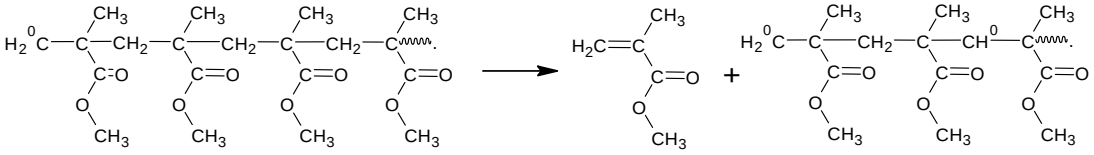

PMMA in radical form — Depolymerization -- (10)

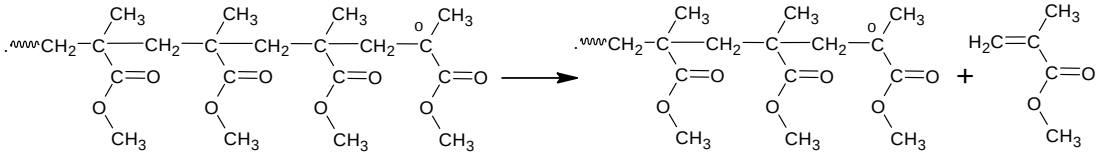

PMMA in radical form — Depolymerization -- (11)

3.5.6. Formation of the adduct, carbonyl, and hydroxyl group.

Free radicals generated in the scheme of reaction (I) interacted with the atmospheric oxygen and formed an adduct. This unstable adduct transforms into carbonyl and hydroxyl groups, as shown in the following scheme of reactions (12), (13), and (14).

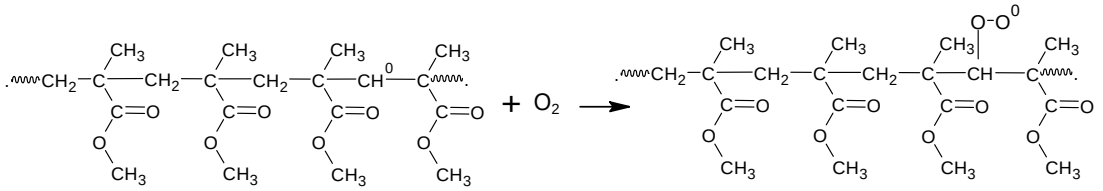

PMMA in radical form — Adduct -- (12)

Adduct formed in the scheme of reaction (13) further transforms into a carbonyl group represented by the scheme of reaction (14). FTIR band peak at 1726 cm^{-1} of the carbonyl group, and its intensity increased due to the rise in the concentration of the carbonyl group (>C=O). The chemical reaction in the scheme of reactions (15) represents the formation of the hydroxyl group, which is observed in the irradiated PMMA polymer reported by a group of researchers [2,51,52,63,64]. However, our study has no significant hydroxyl (O-H) band peak formation, although we noticed slight increases in absorbance in the band range of 3200-3700 cm^{-1}.

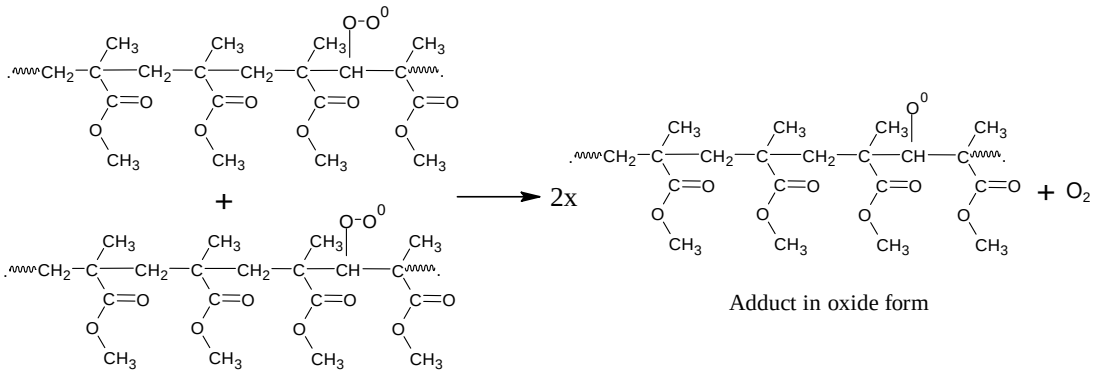

-- (13)

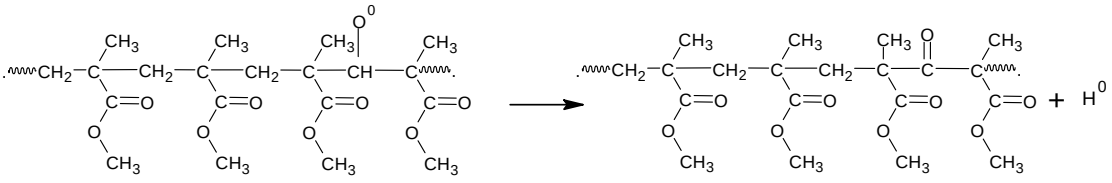

-- (14)

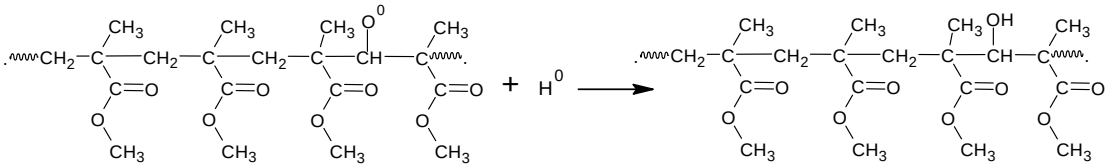

-- (15)

4. Conclusions

The degradation reaction mechanism of the irradiated PMMA polymer has been investigated by using SEM, XRD, FTIR, and UV-Vis spectroscopy. SEM images show no significant change in surface morphology on irradiation up to 570 kGy. X-ray pattern shows that percent crystallinity first decreases from pristine value and then increases with an increase in gamma dose. This is because the generation of free radicals and crosslinking affects crystallinity. The lowest dose (5kGy) of γ-irradiation is effective and enhances optical absorbance detected by UV-Vis spectroscopy. No significant measurable effect of radiation on lattice planes distance. The size of crystallites is moderately affected by radiation. Radiation induces both chain scission and crosslinking in the PMMA polymer. Crosslinking is preferred at a lower dose; however, chain scission is higher. The formation of isosbestic points at wavelengths 325 nm and 373 nm is due to the ratio of absorption and transmission coefficient being unaffected so that the absorbance value remains unchanged. Due to the existence of the isosbestic points in PMMA polymer, it can be used to determine accuracy in the wavelength of the spectrophotometer.

A new absorption band appears in the visible spectral range due to color centers due to the generation of defects in the PMMA polymer after irradiation. Visually coloring of the almost colorless PMMA sample on irradiation from pristine has been observed. Color center and bathochromic shift are due to an increase in the number of conjugation in the irradiated polymer. The band energy gap decreases with an increase in radiation dose. FTIR results ($1635cm^{-1}$) show the development of unsaturated (C=C) centers in the irradiated polymer. The reaction mechanism of products formation chemistry of unsaturation, low molecular weight products, chain scission, crosslinking, dimer PMMA-PMMA, and depolymerization generation has been discussed. The gamma irradiation in the air induces unsaturation hydroxyl group

formation in the irradiated polymer. This modifies the molecular structure of the PMMA polymer.

Funding

The authors thank the TEQIP-III Program, Govt. of India, and the Director, UPTTI, Kanpur, U.P., India, for providing financial support and instrumentation facilities.

Acknowledgments

The corresponding author is thankful to UGC-DAE CSR Kolkata Center, W.B. India, for providing the gamma irradiation facility and to the Head of Department of Chemistry, HBTU, Kanpur, U.P., India, for providing necessary facilities.

Conflicts of Interest

The authors declare no conflict of interest.

References

1. Chapiro, A. General consideration of the radiation chemistry of polymers. *Nucl. Inst. Methods Phys. Res. B* **1995**, *105*, 5–7, https://doi.org/10.1016/0168-583X(95)00861-6.
2. Rai, V.N.; Mukherjee, C.; Jain, B. UV-Vis and FTIR spectroscopy of gamma irradiated polymethyl methacrylate,"*Indian J. Pure Appl. Phys.* **2017**, *55*, 775–785, https://nopr.niscair.res.in/handle/123456789/43118.
3. Ražem, D.; Katušin-Ražem, B. The effects of irradiation on controlled drug delivery/controlled drug release systems. *Radiat. Phys. Chem.* **2008**, *77*, 288–344, https://doi.org/10.1016/j.radphyschem.2007.06.006.
4. O'Donnell J H and Sangester D F, Principles of Radiation Chemistry, Edward Arnold (Publishers) Ltd., London **1970.**
5. Maggi, L.; Segale, L.; Ochoa Machiste, E.; Faucitano, A.; Buttafava, A.; Conte, U. Polymers-gamma ray interaction. Effects of gamma irradiation on modified release drug delivery systems for oral administration. *Int. J. Pharm.***2004**, *269*, 343–351, https://doi.org/10.1016/j.ijpharm.2003.09.027.
6. Burg, K.J.L.; Shalaby, S.W. Radiation Sterilization of Medical Devices and Pharmaceuticals,"*ACS Symp. Ser.***1996**, *620*, 240–245, https://doi.org/10.1021/bk-1996-0620.ch018.
7. Chung, J.P.; Seong, Y.M.; Kim, T.Y.; Choi, Y.; Kim, T.H.; Choi, H.J.; Min, C.H.; Benmakhlouf, H.; Chun, K.J.; Chung, H.T. Development of a PMMA phantom as a practical alternative for quality control of gamma knife dosimetry,"*Radiat. Oncol.***2018**, *13*, 176, https://doi.org/10.1186/s13014-018-1117-8.
8. Polovka M.; Brezova V.; Simko P. EPR spectroscopy: A tool to characterize gamma-irradiated foods, *J. Food Nutr. Res.* **2007**, *46*, 75-83, https://www.researchgate.net/publication/285875655_EPR_spectroscopy_A_tool_to_characterize_gamma-Irradiated_foods.
9. Goulas, A.E.; Riganakos, K.A.; Badeka, A.; Kontominas, M.G. Effect of ionizing radiation on the physicochemical and mechanical properties of commercial monolayer flexible plastics packaging materials. *Food Addit Contam* **2002**, *19*, 1190–1199, https://doi.org/10.1080/0265203021000012402.
10. Manjunatha, H.C. A study of gamma attenuation parameters in poly methyl methacrylate and Kapton. *Radiat. Phys. Chem* .**2017,** *137*, 254–259, https://doi.org/10.1016/j.radphyschem.2016.01.024.
11. Aziz, S.B.; Abdullah, O.G.; Brza, M.A.; Azawy, A.K.; Tahir, D.A.Effect of carbon nano-dots (CNDs) on structural and optical properties of PMMA polymer composite. *Results Phys.* **2019,** *15*, 102776, https://doi.org/10.1016/j.rinp.2019.102776.
12. Zafar, M.S. Prosthodontic applications of polymethyl methacrylate (PMMA): An update. *Polymers* **2020**, *12*, 1–35, https://doi.org/10.3390/polym12102299.
13. Cao, D.; Yang, G.; Bourham, M.; Moneghan, D. Gamma radiation shielding properties of poly (methyl methacrylate)/Bi2O3 composites. *Nucl. Eng. Technol.* **2020**, *52*, 2613–2619, https://doi.org/10.1016/j.net.2020.04.026.

14. Avella, M.; Errico, M.E.; Martuscelli, E. Novel PMMA/CaCO3 Nanocomposites Abrasion Resistant Prepared by an in Situ Polymerization Process. *Nano Lett.* **2001**, *1*, 213–217, https://doi.org/10.1021/nl015518v.
15. Zahid, M.A.; Park, H.; Cho, Y.H.; Yi, J. Plasma etched PMMA/CaF2 anti-reflection coating for light weight PV module. *Opt Mater (Amst)* **2021**, *112*, 110813, https://doi.org/10.1016/j.optmat.2021.110813.
16. Ghosh, P.; Laramore, D.; McGregor, D. S. Characterization and pulse-shape discrimination of a multi-stacked structure of ZnS: Ag/PMMA for fast-neutron detection in high-flux environments. *Nucl Instruments Methods Phys Res Sect A Accel Spectrometers, Detect Assoc Equip*. **2020,** *984*, 164496, https://doi.org/10.1016/j.nima.2020.164496.
17. Karaaslan, H.; Engin, B. ESR dosimetric properties of gamma irradiated different origin eyeglass samples. *Appl Radiat Isot*. **2021**, *178*, 109987, https://doi.org/10.1016/j.apradiso.2021.109987.
18. Romanenko, O.; Slepička, P.; Kvítek, O.; Šlouf, M.; Němecek, P.; Havránek, V.; Macková, A.; Švorčík, V. In-situ generation of Au nanoparticles in poly(methyl methacrylate) films via MeV proton irradiation. *Mater Chem Phys*. **2022**, *275*, 125205, https://doi.org/10.1016/j.matchemphys.2021.125205.
19. Al-Qaradawi, I.Y.; Abdulmalik, D.A.; Madi, N.K.; Almaadeed, M. Gamma irradiation effects on polymethyl methacrylate. in *Physica Status Solidi (C) Current Topics in Solid State Physics*, **2007**, *4*, 3727–3730, https://doi.org/10.1002/pssc.200675846.
20. Silva, P.; Albano, C.; Perera, R.; Domínguez, N. Study of the gamma irradiation effects on the PMMA/HA and PMMA/SW. *Radiat. Phys. Chem.* **2010**, *79*, 358–361, https://doi.org/10.1016/j.radphyschem.2009.08.023.
21. Huszank, R.; Szilágyi, E.; Szoboszlai, Z.; Szikszai, Z. Investigation of chemical changes in PMMA induced by 1.6 MeV He+ irradiation by ion beam analytical methods (RBS-ERDA) and infrared spectroscopy (ATR-FTIR). *Nucl. Inst. Methods Phys. Res. B* **2019**, *450*, 364–368, https://doi.org/10.1016/j.nimb.2018.05.016.
22. Abutalib, M.M.; Rajeh, A. Influence of Fe3O4 nanoparticles on the optical, magnetic and electrical properties of PMMA/PEO composites: Combined FT-IR/DFT for electrochemical applications. *J. Organomet. Chem.* **2020**, *920*, 121348, https://doi.org/10.1016/j.jorganchem.2020.121348.
23. Sharma, A.; Chawla, M.; Gupta, D.; Kumari, R.; Bura, M.; Shekhawat, N.; Aggarwal, S. Low energy B+ implantation induced optical and structural characteristics of aliphatic and aromatic polymers. *Vacuum* **2019**, *159*, 306–314, https://doi.org/10.1016/j.vacuum.2018.10.058.
24. Sakurabayashi, Y.; Masaki, T.; Iwao, T.; Yumoto, M. Surface hardness improvement of PMMA by low-energy ion irradiation and electron irradiation. *Electron. Commun. Japan* **2011**, *94*, 19–26, https://doi.org/10.1002/ecj.10350.
25. Madani, N.; Sardari, D.; Hosntalab, M.; Zobdeh, P. Real time dose rate meter for gamma radiation using LDPE and PMMA in presence of 1–5 kV/mm electric field, *Radiat. Phys. Chem.* **2018**, *151*, 164–168, https://doi.org/10.1016/j.radphyschem.2018.06.002.
26. Lima, V.; Hossain, U.H.; Walbert, T.; Seidl, T.; Ensinger, W. Mass spectrometric comparison of swift heavy ion-induced and anaerobic thermal degradation of polymers. *Radiat. Phys. Chem.* **2018**, *144*, 21–28, https://doi.org/10.1016/j.radphyschem.2017.10.024.
27. Prasad, S.G.; De,A.; De,U. Structural and Optical Investigations of Radiation Damage in Transparent PET Polymer Films. *Int. J. Spectrosc.*, **2011**, *2011*, 1–7, https://doi.org/10.1155/2011/810936.
28. Singh, P.; Ram, J.; Chauhan, V.; Nambissan, P. M. G.; Gupta, S. K.; Kumar, S.; Sharma, S. K.; Sahare, P. D.; Kumar, R. High dose gamma radiation exposure upon Kapton-H polymer for modifications of optical, free volume, structural and chemical properties. *Optik (Stuttg)* **2020**, *205*, 164244, https://doi.org/10.1016/j.ijleo.2020.164244.
29. Singh, P.; Kumar, R.; Cyriac, J.; Rahul, M.T.; Nambissan, P.M.G.; Prasad, R. High energy (MeV) ion fluence dependent nano scale free volume defects studies of PMMA films. *Nucl. Inst. Methods Phys. Res. B* **2014**, *320*, 64–69, https://doi.org/10.1016/j.nimb.2013.11.010.
30. Sinha, D. Structural Modifications of Gamma Irradiated Polymers: An FT-IR Study.*Adv. Appl. Sci. Res.*, **2012,** *3*, 1365–1371.
31. Abdullahi, S.; Aydarous, A.; Salah, N. Fabrication of Alq3/PMMA nanocomposite sheet and its potential applications as radiation dosimeter. *J Lumin*. **2022**, *242*, 118588, https://doi.org/10.1016/j.jlumin.2021.118588.
32. El-Malawy, D.; Al-Abyad, M.; El Ghazaly, M.; Abdel Samad, S.; Hassan, H.E. γ-ray effects on PMMA polymeric sheets doped with CdO nano particles. *Radiat Phys Chem*. **2021**, *184*, 109463, https://doi.org/10.1016/j.radphyschem.2021.109463.

33. Beigzadeh, A.M.; Vaziri, M.R.R. Z-scan dosimetry of gamma-irradiated PMMA. *Nucl Instruments Methods Phys Res Sect A Accel Spectrometers, Detect Assoc Equip.* **2021,** *991*, 165022, https://doi.org/10.1016/j.nima.2021.165022.
34. Prasad, S.G.; Lal, C.; Sahu, K.R.; Saha, A.; De, U. Spectroscopic investigation of degradation reaction mechanism in γ-rays irradiation of HDPE. *Biointerface Res. Appl. Chem.* **2021**, *11*, 9405–9419, https://doi.org/10.33263/BRIAC112.94059419.
35. Alexander P.; Charlesby A.; Ross M. The Degradation of Solid Polymethyl methacrylate by Ionizing Radiation. *Proceed. of the Royal Society of London. Series A, Math. Phys. Scie.* **1954,** *223*, 392-404,https://www.jstor.org/stable/99563.
36. Todd, A. The mechanisms of radiation-induced changes in vinyl polymers. *J. Polym. Sci.* **1960**, *42*, 223–247, https://doi.org/10.1002/pol.1960.1204213925.
37. Ferry, M.; Esnouf, S.; Leprêtre, F.; Cabet, C.; Bender, M.; Severin, D.; Balanzat, E.; Ngono, Y. Effect of oxygen on gas emitted from polymer irradiated using Swift Heavy Ion beams. *Nucl Instruments Methods Phys Res Sect B Beam Interact with Mater Atoms*. **2021**, *497*, 51-58, https://doi.org/10.1016/j.nimb.2021.04.006.
38. Singh, P.; Kumar, R.; Singh, R.; Roychowdhury, A.; Das, D. The influence of crosslinking and clustering upon the nanohole free volume of the SHI and γ-radiation induced polymeric material. *Appl. Surf. Sci.***2015**, *328*, 482–490, https://doi.org/10.1016/j.apsusc.2014.12.065.
39. Samad, R.E.; Courrol, L.C.; Lugão, A.B.; Freitas, A.Z. de; Vieira, N.D. Production of color centers in PMMA by ultrashort laser pulses. *Radiat. Phys. Chem.* **2010**, *79*, 355–357, https://doi.org/10.1016/j.radphyschem.2009.08.017.
40. Klaumünzer, S.; Schnabel, W.; Sotobayashi, H.; Asmussen, F.; Tabata, Y. Linear Energy Transfer Effects in the Radiolysis of Polymers. 1. Main-Chain Degradation of Poly(methyl methacrylate). *Macromolecules* **1984**, *17*, 2108–2111, https://doi.org/10.1021/ma00140a040.
41. Eissa, M.F.; Kaid, M.A.; Kamel, N.A. The influence of low- and high-linear energy transfers on some physical properties of poly(methyl-methacrylate) samples. *J. Appl. Polym. Sci.* **2012,** *125*, 3682–3687, https://doi.org/10.1002/app.36695.
42. Wall, L.A.; Brown, D.W. Chemical Activity of Gamma-Irradiated Poly methyl Methacrylate. *J. Res. Natio. Bur. Stand.***1956,***57*, 131-136, https://nvlpubs.nist.gov›jres›V57.N03.A02.pdf.
43. Ohnishi, S.-I.; Nitta, I.S.-I. Rate of formation and decay of free radicals in γ-irradiated polymethyl methacrylate by means of electron spin resonance absorption measurements. *J. Polym. Sci.* **1959**, *38*, 451–458, https://doi.org/10.1002/pol.1959.1203813416.
44. Hu, Y.H.; Chen, C.Y. The effect of end groups on the thermal degradation of poly(methyl methacrylate). *Polym. Degrad. Stab.***2003**, *82*, 81–88, https://doi.org/10.1016/S0141-3910(03)00165-4.
45. Ramya, J.R.; Arul, K.T.; Sathiamurthi, P.; Nivethaa, E.A.K.; Baskar, S.; Amudha, S.; Mohana, B.; Elayaraja, K.; Chandra Veerla, S.; Asokan, K.; Kalkura, S.N. Gamma irradiated poly (methyl methacrylate)-reduced graphene oxide composite thin films for multifunctional applications. *Compos. Part B Eng.* **2019**, *163*, 752–760, https://doi.org/10.1016/j.compositesb.2019.01.041.
46. Chathuranga, H.; Chandula Wasalathilake, K.; Marriam, I.; MacLeod, J.; Zhang, Z.; Bai, R.; Lei, Z.; Li, Y.; Liu, Y.; Yang, H.; Yan, C. Preparation of bioinspired graphene oxide/PMMA nanocomposite with improved mechanical properties. *Compos Sci Technol*. **2021**, *216*, 109046, https://doi.org/10.1016/j.compscitech.2021.109046.
47. El-Gamal, S.; Elsayed, M. Synthesis, structural, thermal, mechanical, and nano-scale free volume properties of novel PbO/PVC/PMMA nanocomposites. *Polymer (Guildf)*. **2020**, *206*, 122911, https://doi.org/10.1016/j.polymer.2020.122911.
48. Romanenko, O.; Havránek, V.; Malinský, P.; Slepička, P.; Stammers, J.; Švorčík, V.; Macková, A.; Fajstavr, D. Effect of irradiation conditions by swift heavy ions on the microstructure and composition of PMMA. *Nucl. Inst. Methods Phys. Res. B*, **2019**, *461*, 175–180, https://doi.org/10.1016/j.nimb.2019.09.043.
49. Jebur, J.H.; Hassan, Q.M.A.; Al-Mudhaffer, M.F.; Al-Asadi, A.S.; Elias, R.S.; Saeed, B.A.; Emshary, C.A. The gamma radiation effect on the surface morphology and optical properties of alpha-methyl curcumin: PMMA film. *Phys. Scr.* **2020,** *95*, 045804, https://doi.org/10.1088/1402-4896/ab5ca0.
50. Alwan, T.J. Effects of gamma irradiation on the physical properties of PAni.MWCNT/PMMA films. *J. Phys. Stud.*, **2019,** *23*, 3710, https://doi.org/10.30970/jps.23.3710.

51. Ennis, C.P.; Kaiser, R.I. Mechanistical studies on the electron-induced degradation of polymethylmethacrylate and Kapton. *Phys. Chem. Chem. Phys.* **2010**, *12*, 14902–14915, https://doi.org/10.1039/c0cp01130d.
52. Tiwari, P.; Srivastava, A.K.; Khattak, B.Q.; Verma, S.; Upadhyay, A.; Sinha, A.K.; Ganguli, T.; Lodha, G. S.; Deb, S.K. Structural modification of poly (methyl methacrylate) due to electron irradiation. *Meas. J. Int. Meas. Confed.* **2014,** *51*, 1–8, https://doi.org/10.1016/j.measurement.2014.01.017.
53. Blout, E.R.; Fields, M. Absorption Spectra. V. The Ultraviolet and Visible Spectra of Certain Polyene Aldehydes and Polyene Azines.*J. Am. Chem. Soc.***1948,** *70*, 189–193, https://doi.org/10.1021/ja01181a055.
54. Che, M.; Védrine, J.C. *Characterization of Solid Materials and Heterogeneous Catalysts: From Structure to Surface Reactivity*, Weinheim, Germany: Wiley-VCH Verlag GmbH & Co. KGaA **2012**, *1*, 97, https://doi.org/10.1002/9783527645329.
55. Tauc, J.; Grigorovici, R.; Vancu, A. Optical Properties and Electronic Structure of Amorphous Germanium. *Phys. status solidi* **1966,** *15*, 627–637, https://doi.org/10.1002/pssb.19660150224.
56. Higazy, A.A.; Hussein, A. Optical absorption studies of γ-irradiated magnesium phosphate glasses. *Radiat. Eff. Defects Solids* **1995,** *133*, 225–235, https://doi.org/10.1080/10420159508223993.
57. Sindhu, S.; Sanghi, S.; Agarwal, A.; Seth, V.P.; Kishore, N. Structural, optical, physical and electrical properties of V2O5·SrO·B2O3 glasses. *Spectrochim. Acta - Part A Mol. Biomol. Spectrosc.***2006,** *64*, 196–204,https://doi.org/10.1016/j.saa.2005.06.039.
58. Chapiro, A. Chemical modifications in irradiated polymers. *Nucl. Inst. Methods Phys. Res. B* **1988,** *32*, 111–114, https://doi.org/10.1016/0168-583X(88)90191-7.
59. Dorey, S.; Gaston, F.; Girard-Perier, N.; Dupuy, N.; Marque, S.R.A.; Delaunay, L. Generation of O2-Permeation Barrier during the Gamma-Irradiation of Polyethylene/Ethylene-Vinyl Alcohol/Polyethylene Multilayer Film. *Ind. Eng. Chem. Res.***2019**, *58*, 14115–14123, https://doi.org/10.1021/acs.iecr.9b02145.
60. Davenas, J; Stevenson, I; Celette, N; Cambon, S; Gardette, J L; Rivaton, A; Vignoud, L. Stability of polymers under ionising radiation: The many faces of radiation interactions with polymers. *Nucl. Inst. Methods Phys. Res. B* **2002,** *191*, 653–661, https://doi.org/10.1016/S0168-583X(02)00628-6.
61. Sinha, D.; Swu, T.; Trieathy, S.P.; Mishra, R.; Dwivedi, K.K.; Fink, D. Spectroscopic and thermal studies of gamma irradiated polypropylene polymer. *Radiat. Eff. Defects Solids* **2003,** *158*, 531–538, https://doi.org/10.1080/1042015031000074101.
62. Lee, E.H.; Rao, G.R.; Mansur, L.K. LET effect on crosslinking and scission mechanisms of PMMA during irradiation. *Radiat. Phys. Chem.***1999,** *55*, 293–305, https://doi.org/10.1016/S0969-806X(99)00184-X.
63. Ismayil; Ravindrachary, V.; Bhajantri, R.F.; Praveena, S.D.; Poojary,B.; Dutta,D.; Pujari, P.K. Optical and microstructural studies on electron irradiated PMMA: A positron annihilation study. *Polym. Degrad. Stab.* **2010,** *95*, 1083–1091, https://doi.org/10.1016/j.polymdegradstab.2010.02.031.
64. Ismayil; Ravindrachary, V.; Praveena, S.D.; Mahesha, M.G. Free volume modifications in chalcone chromophore doped PMMA films by electron irradiation: Positron annihilation study. *Radiat. Phys. Chem.* **2018**, *144*, 194-203, https://doi.org/10.1016/j.radphyschem.2017.08.015.
65. Valente, C.J.; Schellenberger, A.M.; Tillman, E.S. Dimerization of Poly(methyl methacrylate) Chains Using Radical Trap-Assisted Atom Transfer Radical Coupling. *Macromolecules* **2014,** *47*, 2226–2232, https://doi.org/10.1021/ma5001805.